

A Layer Selection Approach to Test Time Adaptation

Sabyasachi Sahoo^{1,2}, Mostafa ElAraby^{2,3}, Jonas Ngnawe^{1,2}, Yann Batiste Pequignot¹,
Frédéric Precioso⁴, Christian Gagné^{1,2,5}

¹IID, Université Laval

²Mila

³Université de Montréal

⁴Université Cote d'Azur, CNRS, INRIA, I3S, Maasai

⁵Canada CIFAR AI Chair

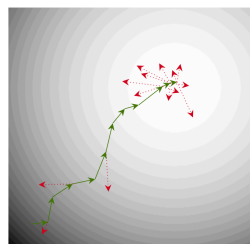
sabyasachi.sahoo.1@ulaval.ca

Abstract

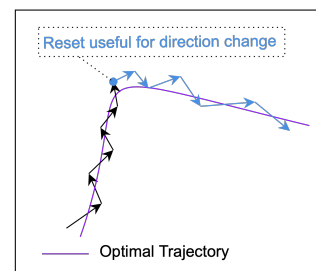
Test Time Adaptation (TTA) addresses the problem of distribution shift by adapting a pretrained model to a new domain during inference. When faced with challenging shifts, most methods collapse and perform worse than the original pretrained model. In this paper, we find that not all layers are equally receptive to the adaptation, and the layers with the most misaligned gradients often cause performance degradation. To address this, we propose GALA, a novel layer selection criterion to identify the most beneficial updates to perform during test time adaptation. This criterion can also filter out unreliable samples with noisy gradients. Its simplicity allows seamless integration with existing TTA loss functions, thereby preventing degradation and focusing adaptation on the most trainable layers. This approach also helps to regularize adaptation to preserve the pretrained features, which are crucial for handling unseen domains. Through extensive experiments, we demonstrate that the proposed layer selection framework improves the performance of existing TTA approaches across multiple datasets, domain shifts, model architectures, and TTA losses.

1 Introduction

Distribution shifts (Gulrajani and Lopez-Paz 2021) present significant challenges when deploying deep learning models in real-world scenarios. Test Time Adaptation (TTA) (Liang, He, and Tan 2023) has emerged as a promising approach for adapting pretrained models to novel domains during inference. However, these methods often falter when confronted with severe or diverse distributional changes. To mitigate potential performance degradation, various regularization strategies have been proposed (Niu et al. 2022; Shin et al. 2024). Nevertheless, these strategies might not effectively address all types of shifts or TTA losses (Burns and Steinhardt 2021; Zhao et al. 2023a). Moreover, the selection of layers in the existing TTA approaches typically remains unchanged across different shifts (Wang et al. 2024), which may not be optimal. In contrast, layer selection has demonstrated substantial improvements in related fields such as domain generalization (Chattopadhyay, Balaji, and Hoffman 2020), fine-tuning (Lee et al. 2023), multi-task learning (Wallingford et al. 2022), and continual learning (Zhao et al.



(a) Gradient alignment



(b) Helpful reset

Figure 1: Intuition for proposed approaches: **(a)** As the model reaches closer to minima, the individual sample gradients start to be misaligned with gradients of previous samples (Mahsereci et al. 2017; Forouzes and Thiran 2021; Agarwal, D'souza, and Hooker 2022). We leverage this misalignment to identify trainable layers. **(b)** While effective in moving in the direction of most aligned gradients, the introduced criterion based on angular deviation could prevent adaptation when a direction change is needed, even if the following updates (or gradients) are aligned. A reset of the past horizon (i.e., gradients of previous samples) considered in the alignment condition can help resolve such situations.

2023b), underscoring the importance and broad potential of layer selection. Still, the question of optimal layer selection remains largely unexplored in the context of TTA.

In this paper, we study layer selection for TTA and show that not all layers of a given model are equally receptive to adaptation. Our findings suggest that adapting the right layer can lead to meaningful improvement, while adapting the wrong layer can cause significant performance degradation in TTA approaches. Specifically, we find that while adapting a certain layer may benefit one shift, it may be detrimental to another. Additionally, we find that on a given shift, the effect of adapting a certain layer also depends on the loss used. Therefore, while we observe an important potential in selecting the right layer to adapt in each situation, identifying these layers at test time can be challenging.

To address the challenges of layer selection, we propose Gradient-Aligned Layer Adaptation, GALA, a novel criterion to identify good layers for adaptation at test time.

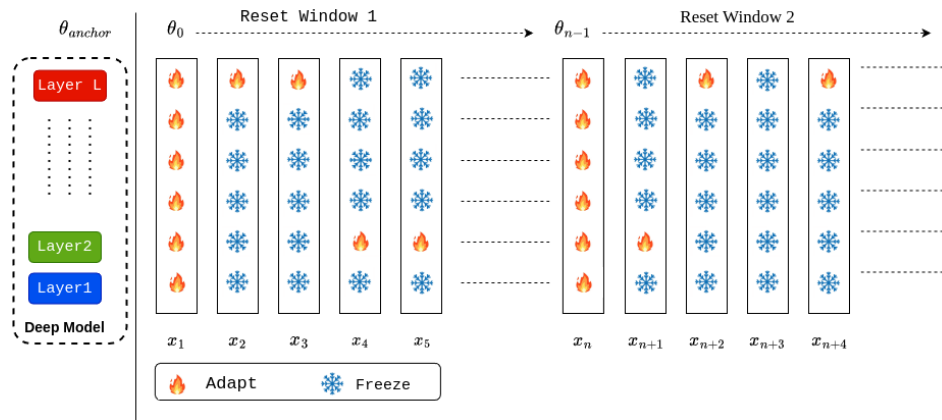


Figure 2: Gradient-Aligned Layer Adaptation or GALA framework adapts the most gradient-aligned layer per sample. It adapts all the layers for the first sample in a reset window (e.g., x_1, x_n, \dots). For all the other samples, it adapts the most gradient-aligned layer per sample. It can also skip the adaptation on a given sample if all the layers are misaligned. We use a reset window to periodically reset the anchor parameters to allow for a change in direction.

GALA ranks all the layers of a model based on the gradient alignment of the current adaptation step. As the model approaches the optimization minima, the variance in gradient updates increases (Mahsereci et al. 2017; Forouzesh and Thiran 2021; Agarwal, D’souza, and Hooker 2022), leading to potential overfitting and performance degradation. Building on this insight, for each layer, we propose to measure the angle deviation of the proposed gradient update from the average of all gradient updates performed so far (including the proposed one). This measure can also be expressed as the cosine between the proposed update and the (anticipated) total displacement of the parameters from their pretrained values. This allows us to compare the updates for each layer on a common scale and only perform the update of the layer with the smallest angle.

Our extensive experiments on Domainbed (Gulrajani and Lopez-Paz 2021) and Continual TTA benchmark (Wang et al. 2022) demonstrate that GALA consistently surpasses *all layers* and *ERM* (no adaptation) baselines and other existing layer selection baselines across various datasets, various neural network backbones, and various losses. Further analysis reveals that GALA can identify the good layers, which exhibit significant displacement in a single direction and higher gradient alignment. This layer selection strategy enhances the model’s ability to adapt to novel domains by mitigating performance degradation and potentially serves as a regularization mechanism, reducing catastrophic forgetting of source domain knowledge. Ablation studies reveal that GALA’s performance is robust to hyperparameter choices.

The contributions of our paper are summarized as follows:

1. We study the problem of layer selection for TTA and find that while adapting specific layers can enhance performance, the optimal set of layers for adaptation is not universal but rather contingent upon the particular distribution shift encountered and the TTA loss function employed during inference.

2. We introduce GALA, a novel layer selection criterion to identify good layers to adapt per sample that can be applied across various distribution shifts and TTA loss functions at test time.
3. Through extensive experiments across different backbones, datasets, and TTA losses, we show that GALA outperforms standard *ERM* (no adaptation), *all layers* baselines, and other layer selection baselines (i.e., AutoRGN and AutoSNR (Lee et al. 2023)) for TTA.

2 Proposed Approach

In the following, we describe the Gradient-Aligned Layer Adaptation (GALA) framework for Test Time Adaptation (TTA). We first introduce our layer selection framework for TTA (Sec. 2.1), before describing the cosine distance criterion proposed to identify the most trainable layers (Sec. 2.2), and then present the reset window strategy used to improve performances with the proposed cosine criterion (Sec. 2.3).

2.1 Layer selection framework for TTA

Let $f_{\theta_{\text{src}}}$ denote the model parameterized by parameters θ_{src} trained beforehand on the source domain \mathcal{D}_{src} . Let us also assume that target domain samples $\{x_i\}_{i=1}^n$ are coming in an online fashion at test time. For some sample x_i at test time, TTA adapts the model to obtain θ_i before performing inference (Sun et al. 2020b; Liang, He, and Tan 2023). We set $\theta_0 = \theta_{\text{src}}$ and, at each step, θ_i is obtained by updating θ_{i-1} using the following equation:

$$\theta_i = \theta_{i-1} + \mathbf{u}_i, \quad (1)$$

where \mathbf{u}_i is a parameter update specific to the TTA algorithm. Typically, if SGD optimizer is used with learning rate η , this update takes the form $\mathbf{u}_i = -\eta \nabla \mathcal{L}(x_i; \theta_{i-1})$, where \mathcal{L} is the unsupervised loss specific to the TTA method.

In this section, we consider single-step TTA performed online on a single input sample using an SGD optimizer for

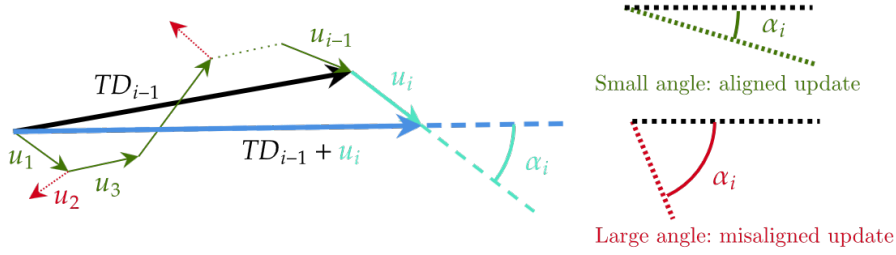


Figure 3: Illustration of proposed criterion based on angular deviation. Different layers can be ranked based on their alignments with previous gradient updates. In the figure, updates drawn in red are discarded, while green updates are applied, adding up to \mathbf{TD}_{i-1} . The update under scrutiny \mathbf{u}_i is drawn in cyan, and its sum with \mathbf{TD}_{i-1} is drawn in blue. Application of update \mathbf{u}_i or not is based on the angle α_i .

notation simplicity. Throughout, we assume the deep learning model is written as a certain composition of functions, which we simply refer to as layers, though any granularity would do. This allows us to write the model at step i as $f_{\theta_i} = f_{\theta_{i,L}} \circ \dots \circ f_{\theta_{i,1}}$, where $\theta_{i,l}$ denote the parameters of layer l at step i . The update equation at step i can be written for each layer as:

$$\theta_{i,l} = \theta_{i-1,l} + \mathbf{u}_{i,l}. \quad (2)$$

To perform layer selection, we modify this update equation by introducing a mask:

$$\theta_{i,l} = \theta_{i-1,l} + m_{i,l} \mathbf{u}_{i,l}, \quad (3)$$

where $m_{i,l} \in \{0, 1\}$ is the value of the binary mask applied to the update $\mathbf{u}_{i,l}$.

2.2 Cosine distance criterion

Existing works have shown that gradient descent happens in a tiny subspace (Gur-Ari, Roberts, and Dyer 2018). Moreover, as the model reaches closer to the minima, the gradients across the samples get noisy (Mahseeraci et al. 2017; Forouzesh and Thiran 2021; Agarwal, D’souza, and Hooker 2022). We aim to identify the layers with the most beneficial gradient updates to the model for adapting to the new domain. Let us assume that the total displacement of parameters of layer l at the start of the i^{th} step is given by:

$$\mathbf{TD}_{i-1,l} = \sum_{j=1}^{i-1} m_{j,l} \mathbf{u}_{j,l} = \theta_{i-1,l} - \theta_{0,l}. \quad (4)$$

Our proposed criterion relies on the angular deviation of the update $\mathbf{u}_{i,l}$ from the direction of the total displacement that would result from making this update:

$$\cos(\alpha_{i,l}) = \frac{\mathbf{u}_{i,l} \cdot (\mathbf{u}_{i,l} + \mathbf{TD}_{i-1,l})}{\|\mathbf{u}_{i,l}\|_2 \|\mathbf{u}_{i,l} + \mathbf{TD}_{i-1,l}\|_2}. \quad (5)$$

This angle can be interpreted as the deviation of the update under consideration from the anticipated average update, which has the same direction as the anticipated total displacement $\mathbf{u}_{i,l} + \mathbf{TD}_{i-1,l}$ – see this illustrated in Fig. 3.

Comparing our criterion across layers allows us to define which update is performed by defining the mask:

$$m_{i,l} = \begin{cases} 1 & \text{if } \cos(\alpha_{i,l}) > \lambda \\ 0 & \text{otherwise} \end{cases}, \quad (6)$$

where λ is the selection threshold. The fact that the cosine metric lies in the $[-1, 1]$ domain allows us to compare the alignment of updates for layers with different sizes of parameters. We set a single $\lambda > 0$ for thresholding over all layers, which prevents the adaptation of updates that are misaligned with the updates applied in the past. A λ close to 1 will only allow adaptation of updates aligned with past updates, while a lower λ would be less restrictive.

2.3 Cosine distance with reset

While the cosine distance can stop adaptation for noisy gradients, our criterion may fail, especially when the gradient update trajectory needs to change direction after a certain point. If the gradient updates meet an inflection point in the loss landscape, cosine distance will prevent further adaptation, and the model will remain stuck at this point even if the gradient update is informative. To solve such cases, we propose to use resets for the computation of the total displacement of a layer. We use a fixed window scheme for resetting the initial parameter point, which we will call the *anchor point*. This corresponds to:

$$\mathbf{TD}_{i,l} = \theta_{i,l} - \theta_{r,l}, \quad (7)$$

where $\theta_{r,l}$ is the parameter at last reset step $r = \lfloor \frac{i-1}{s} \rfloor$, and s is the size of the reset window. The anchor point changes only when the reset window changes, as illustrated in Fig. 2.

3 Experiments

This section compares our proposed approaches with existing baselines on Domainbed (Gulrajani and Lopez-Paz 2021), a popular benchmark with large single distribution shifts, and Continual TTA, a popular benchmark with multiple distribution shifts.

TTA losses Two popular TTA losses are considered: Pseudo-Labeling (PL) (Lee et al. 2013) and SHOT (Liang, Hu, and Feng 2020). We perform hyperparameter selection based on Zhao et al. (2023a), where we report the performance for the best hyperparameter set found by sweeping over a range of values.

Baselines We compare the TTA performance obtained by adapting *All layers* vs. the layers proposed by our approach. We also report the *ERM (no adaptation)* performance of the

TTA	Method	PACS \uparrow	VLCS \uparrow	Terra \uparrow	Office \uparrow	Mean \uparrow	
ResNet-18	ERM -	80.99 (± 0.9)	75.14 (± 1.2)	40.80 (± 0.2)	62.18 (± 0.4)	64.78	
	PL	All layers	81.79 (± 0.7)	65.69 (± 1.5)	35.40 (± 9.7)	60.20 (± 1.4)	60.77
		AutoRGN	82.82 (± 0.6)	72.63 (± 1.3)	38.18 (± 6.1)	62.38 (± 0.2)	64.00
		AutoSNR	80.58 (± 1.2)	65.72 (± 1.8)	35.01 (± 10.4)	59.82 (± 0.9)	60.28
		GALA	83.56 (± 0.6)	75.48 (± 1.2)	44.19 (± 1.1)	62.67 (± 0.2)	66.47
	SHOT	All layers	83.48 (± 0.3)	66.23 (± 2.8)	33.81 (± 1.3)	63.03 (± 0.4)	61.64
		AutoRGN	84.10 (± 0.5)	69.78 (± 1.3)	37.37 (± 0.7)	63.09 (± 0.2)	63.59
		AutoSNR	83.43 (± 0.3)	66.26 (± 2.7)	33.75 (± 1.2)	63.02 (± 0.4)	61.62
		GALA	83.92 (± 0.8)	76.23 (± 1.1)	42.13 (± 1.4)	63.32 (± 0.3)	66.40
	ResNet-50	ERM -	82.84 (± 0.5)	75.83 (± 0.9)	46.14 (± 2.3)	66.93 (± 0.3)	67.93
PL		All layers	82.36 (± 2.8)	69.22 (± 1.4)	42.28 (± 3.2)	61.54 (± 3.3)	63.85
		AutoRGN	85.03 (± 1.9)	75.35 (± 1.4)	48.44 (± 2.4)	66.93 (± 0.3)	68.94
		AutoSNR	83.41 (± 3.4)	70.14 (± 4.6)	44.08 (± 3.4)	61.95 (± 3.0)	64.90
		GALA	84.87 (± 0.8)	76.88 (± 1.6)	50.10 (± 2.5)	67.34 (± 0.3)	69.80
SHOT		All layers	85.15 (± 1.1)	64.25 (± 1.1)	35.33 (± 3.1)	67.37 (± 0.3)	63.03
		AutoRGN	86.34 (± 1.1)	70.2 (± 0.9)	40.59 (± 1.3)	68.10 (± 0.4)	66.31
		AutoSNR	85.51 (± 0.5)	64.26 (± 1.3)	34.97 (± 3.2)	67.33 (± 0.2)	63.02
		GALA	86.13 (± 0.8)	76.48 (± 1.0)	45.94 (± 1.6)	68.13 (± 0.3)	69.17

Table 1: Accuracy (%) of various layer selection methods on Domainbed benchmark (setup described in Sec. 3.1). The best method for a given TTA loss and backbone is in bold.

pretrained model. In Domainbed, we also compare against AutoRGN and AutoSNR (Lee et al. 2023), two popular baselines proposed to identify optimal layers in fine-tuning setup.

Implementational details We report results for GALA with *window size* of 20 and *selection threshold* of 0.75 with single-layer granularity. It appears that GALA is not overly sensitive to hyperparameters, and those values work well overall – see Sec. 5 for more discussion on hyperparameter values and the design choices. We also scale the updates for a few initial samples in the reset window to reduce their impact on incorrect layer selection.

3.1 Domainbed results

For the experiments on Domainbed, we follow the evaluation protocol as described in Iwasawa and Matsuo (2021), including dataset splits for the following four datasets: PACS (Li et al. 2017), VLCS (Fang, Xu, and Rockmore 2013), Terra Incognita (Beery, Van Horn, and Perona 2018), and Office-Home (Venkateswara et al. 2017). Results are reported on two backbones (i.e., ResNet-18 and ResNet-50) with batch normalization layers, while the pretrained models are made using default hyperparameters described in Gulrajani and Lopez-Paz (2021). Mean and standard deviation are reported over three repetitions with different random seeds. See Appendix A.2 for further details.

Key takeaways from results are reported in Tab. 1:

- GALA outperforms ERM (no adaptation) by 2% overall and *All layers* TTA baselines by more than 5% overall across all losses, backbones, and datasets.
- Existing layer selection baselines like AutoRGN or AutoSNR can improve performance compared to all layers TTA in most setups, especially AutoRGN, but fail to improve against no adaptation baselines for some datasets like VLCS or TerraIncognita or some TTA losses like SHOT. GALA consistently demonstrates equivalent or superior performance across all datasets and TTA losses, achieving an overall improvement of about 2%.

TTA	Method	CIFAR10C \downarrow	CIFAR100C \downarrow
ERM		43.50 (± 18.7)	46.40 (± 15.7)
PL	All layers	88.72 (± 1.2)	98.63 (± 1.5)
	GALA	28.68 (± 6.6)	33.69 (± 5.7)
SHOT	All layers	89.33 (± 2.3)	97.32 (± 4.8)
	GALA	20.46 (± 7.7)	32.87 (± 5.6)

Table 2: Accuracy (%) of layer selection methods on Continual TTA benchmark (with the setup described in Sec. 3.2). The best method for a given TTA loss is in bold.

- GALA improves over Domainbed large shift datasets (i.e., PACS, OfficeHome) similar to AutoRGN and AutoSNR while comfortably outperforming the ERM baseline. On small shift datasets (i.e., VLCS, TerraIncognita), existing baselines struggle to outperform the *no adaptation* baseline while GALA appears to prevent degradation caused by over-adaptation, thereby enhancing performance over the ERM baseline and safeguard against further degradation.

3.2 Continual TTA results

We follow the evaluation protocol as described in Wang et al. (2022), evaluating performance on two datasets-backbones: 1) CIFAR10C (Hendrycks and Dietterich 2019) with WideResNet-28 (Zagoruyko and Komodakis 2016) and CIFAR100C (Hendrycks and Dietterich 2019) with ResNeXt-29 (Xie et al. 2017). The pretrained models are trained as described in Robustbench (Croce et al. 2021). Mean and standard deviation are reported across the 15 corruption types. Further details are given in Appendix A.3.

The key takeaways based on the results from Tab. 2 are:

- Performance degradation by training all layers is worse in the Continual TTA benchmark containing multi-domain shifts than degradation in the Domainbed benchmark containing single-domain shifts. Moreover, more severe degradations are observed in CIFAR100C, which has 100 classes, compared to CIFAR10, which includes 10 classes, despite similar ERM performance on both datasets.
- GALA consistently outperforms ERM by about 15% and all layers TTA baseline by about 65%, despite severe degradation.

4 Layer Selection Study

In this section, we evaluate the importance of layer selection for test time adaptation on the Domainbed benchmark and provide some analysis and motivation for GALA. We use the Domainbed benchmark with the ResNet-18 backbone, which contains four blocks of layers. We study the effect of choosing one block over another by performing adaptation on a single block while freezing all the other blocks of the model. We refer to blocks and layers interchangeably in this section. We report the difference between TTA and ERM accuracy over all blocks for each loss and dataset shift setting. Otherwise, we rely on the same setup and evaluation protocol described in Sec. 3.1.

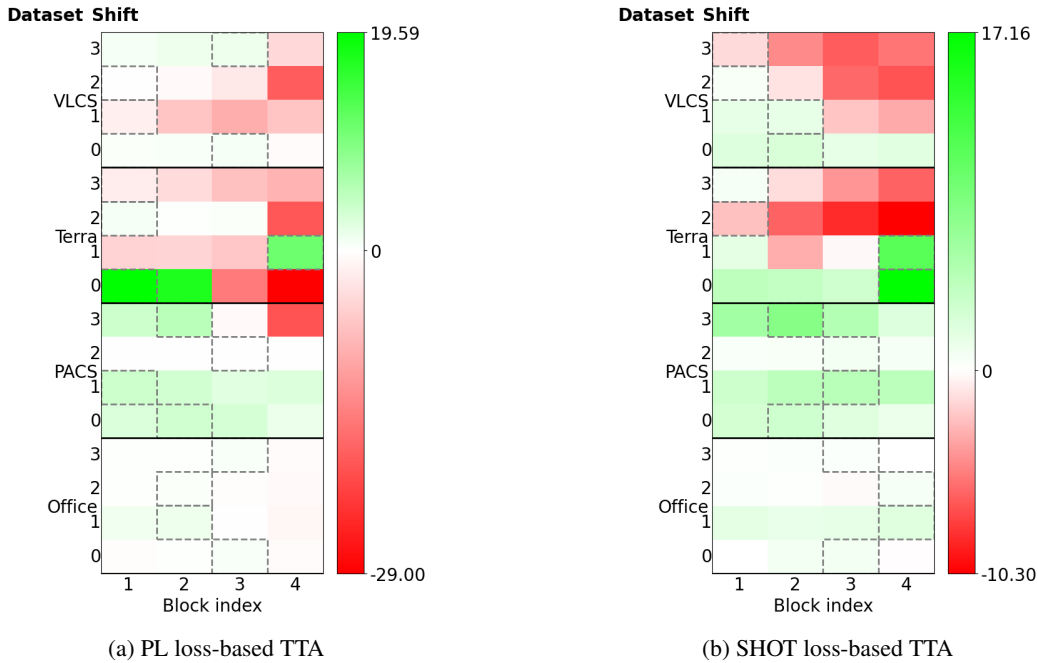


Figure 4: Heatmap of Performance improvement (%) per-block on Domainbed benchmark. Performance improvement is the difference between the TTA accuracy of a given block/layer and ERM accuracy for the same shift. Positive performance improvements are shown in green, and negative performance improvements (or degradation) are in red. Using the bounding box, we highlight the best block per loss and dataset shift. Further details in Sec. 4.

4.1 Layer selection matters

In Fig. 4, we observe that not all layers are equally receptive to adaptation. We refer to a layer as good or bad based on the accuracy improvement of selecting a given layer w.r.t. performance of a pretrained model on the same shift. We compare against Empirical Risk Minimization (ERM) or the frozen pretrained model’s performances, as we are interested in measuring the performance improvement or degradation brought by individual layers during adaptation. Also, the ERM model performs better on average than *all layer* TTA, as seen in Sec. 3, and it becomes a natural baseline that can help contrast different layers.

The selection of layers in existing TTA approaches typically remains unchanged in all adaptation settings. We find it can be a suboptimal strategy and one of the major causes of degradation in existing TTA approaches – no single layer adaptation is suitable for all settings. Therefore, layer selection is essential for TTA, and we propose GALA to improve the performance of existing TTA approaches in various settings.

4.2 What affects the adaptability of a layer?

Using the same setup and evaluation protocol (cf., Sec. 3.1), we are making the following observations on Fig. 4 about the factors affecting the adaptability of good layers:

- Location of good layers in a model can change across shifts of a given dataset, despite using pretrained models trained on the same class labels. Similar observations have also been made in fine-tuning setups (Lee et al.

2023). There is a need for a good layer selection criterion that depends on target samples observed by the model at test time.

- We also find that good layers in a model can change with different TTA loss functions, even for the same shift and dataset. Hence, a good layer selection criterion must also depend on the TTA loss function used to adapt the model at inference.

Since gradients depend on the shift and TTA loss function used, GALA uses layerwise gradients to identify the adaptability of each layer in the model.

4.3 How do good layers differ from bad layers?

To perform a detailed per-layer analysis, we created the Tiny-Domainbed benchmark, which was made as a smaller version of Domainbed. It consists of all the critical shifts with the brightest red/green layers (displayed in Fig. 4), whose good layers can also change with the TTA method. We follow the benchmark and evaluation protocol described in Sec. 3.1, with further details given in Appendix A.4. Based on Tab. 3, the following are the differences between good and bad layers:

- Adaptation with *Worst Block* results in poor TTA accuracy, poorer generalization to the target domain, and higher forgetting. Since training all layers involves training the worst layer, this could explain why training all layers results in poorer TTA accuracy. On the other hand, *Best Block* results in better generalization to the target domain. This implies that TTA with good layers can poten-

Method	TTA Acc. \uparrow	Gen. \uparrow	Forget. \downarrow	Rank corr. \uparrow
All Blocks	53.6	46.5	31.3	N/A
Worst Block (oracle)	43.5	38.7	39.9	-1
Best Block (oracle)	64.1	63.9	28.7	1
Random Block	53.1	49.1	<u>13.1</u>	0
GALA	<u>59.4</u>	<u>58.0</u>	9.3	<u>0.76</u>

Table 3: Effect of various layer selection methods on TTA Accuracy (%), Generalization (%), Forgetting (%) and Spearman correlation with Best Block ($\in [-1, 1]$) averaged over different shifts on Tiny-Domainbed benchmark (with the setup described in Sec. 4.3). *TTA Acc* is the accuracy of testing samples from the target domain seen during adaptation. *Generalization* is the accuracy of the held-out split of the target domain after adaptation. *Forgetting* is the drop in accuracy on the held-out split of source domains after adaptation. *Rank correlation* is the Spearman correlation of layer selection rank between the oracle and the method. Bold and underlined denote best and second-best, respectively.

tially learn target domain features better than TTA with bad layers.

- We observe that *Best Block* results in reduced source forgetting compared to *Worst Block*. This implies that TTA with good layers strikes an improved balance between learning new features on the target domain while retaining useful pretrained features from the source domain.

Therefore, we propose GALA to identify good layers for adaptation, which can help balance adaptation to the new domain while reducing source forgetting.

4.4 How does GALA compare to oracle strategies?

To analyze GALA’s layer selection behavior, we compare it to the oracle strategies given by Best block and Worst block on the Tiny-Domainbed benchmark (Tab. 3).

GALA well approximates the oracle layer selection GALA substantially improves over *All Blocks*, *Worst Block*, and *Random Block* method. In some sense, *Best Block* method acts as an empirical upper-bound performance if we have access to a target domain with labels while incurring the high computational cost of brute forcing over individual layers of the model. GALA comes close to this upper bound performance without requiring any target labels using a cheap layer selection criterion. As a result, GALA also effectively balances computational cost with performance.

GALA is more conservative than the oracle GALA selects the layers for adaptation with the most aligned gradients. It can stop adaptation if the gradients are noisy or no longer aligned to prevent further degradation. In Tab. 3, we see that it may have aggressively stopped a few useful updates compared to the *Best Block*, our empirical upper bound. As a result, it gets much better at avoiding forgetting but is a bit lower on TTA accuracy and generalization.

GALA tends to select more often the blocks with better accuracy Oracle TTA performance, as measured in Fig. 4, ranks the four blocks for each configuration. Similarly,

Setting	Condition	Accuracy \uparrow
Partitioning	Single block	67.64
	Single layer	68.57
	Multiple layers	66.48
Window Size	5	68.46
	20	68.57
	∞	68.37
Threshold	0.5	68.57
	0.75	68.57
	0.99	68.6
Batch Size = 1	All Layers	33.47
	GALA	67.28
Continual TTA	No Reset	69.9
	With Reset	71.1

Table 4: Accuracy (%) under different experimental conditions. The values are averaged on Domainbed for the first four settings and Continual TTA for the last.

GALA chooses to update each layer with a particular frequency during TTA, leading to a ranking of the four blocks. We assess the relationship between these two different ways of ranking blocks using Spearman rank correlation and find $\rho = 0.76$ (cf. Tab. 3), which seems to indicate that the selection strategy used by GALA is a good proxy for the oracle TTA performance achieved when adapting always the same layer.

5 Analysis of GALA

In this section, we evaluate the impact of different design choices and hyperparameters of GALA in Tab. 4, supporting choices presented in Tab. 1. For the partitioning setting, *Single block* means a single block of many layers is updated at each iteration, *Single layer* corresponds to the best layer selected for the update, and *Multiple layers* corresponds to individually best layers selected for the update based on the cosine distance and the threshold. Also, a window size of ∞ implies no reset. Some important observations stemming from Tab. 4:

- Layer granularity performs better than block granularity. At layer granularity, GALA has better fine-grained control over choosing the layers to adapt, improving performances in all cases tested.
- Adaptation with the best single layer is much better than with the best multiple layers. Cosine distance can correctly identify the single best layer to train, although it may still struggle to determine the best set of multiple layers to update.
- Optimal reset-window size can improve performance. We see that a reset window size of 20 works reasonably well across the backbones and the TTA losses tested on Domainbed.
- The choice of selection threshold is not very sensitive. A threshold of 0.75 seems to work across the board without being too restrictive.

In the following section, we briefly analyze some aspects of the proposed approach.

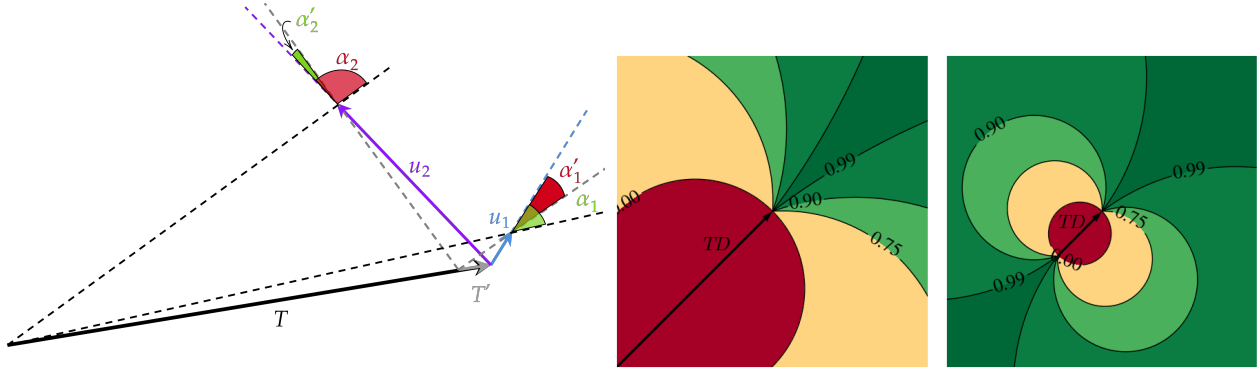


Figure 5: Effect of magnitude of u on cosine distance criterion. **Left:** Consider two vectors such that u_1 is smaller than u_2 but is better aligned with its displacement. For large displacements (T), alignment becomes crucial and GALA selects u_2 . For small displacements (T'), the update’s magnitude can dominate the criterion, and GALA selects u_1 . **Middle and Right:** Plot of cosine metric values with level curves. Alignment prevails for small updates compared to the total displacement (Middle). But, for updates with large magnitude compared to total displacement (Right), large cosine values can be obtained even for misaligned updates.

Proposed cosine distance criterion effectively balances gradient magnitude and direction. Let us first rewrite the GALA criterion in Eq. 5 for a given layer l in terms of $T = \|\mathbf{TD}_{i-1,l}\|$, $u = \|\mathbf{u}_{i,l}\|$ and the angle β between $\mathbf{TD}_{i-1,l}$ and $\mathbf{u}_{i,l}$. Using the Pythagorean theorem, we obtain:

$$\cos(\alpha) = \frac{T \cos(\beta) + u}{\sqrt{(T + u \cos(\beta))^2 + (u \sin(\beta))^2}}. \quad (8)$$

We observe that our criterion depends on the norm T of the total displacement, the norm u of the update, and their alignment, given by the angle β between these vectors. Fig. 5 shows the cosine metric plots. We see that while alignment is crucial for large displacements, the update’s magnitude can also dominate for small displacements. For example, consider two layers with the same norm T but different updates \mathbf{u}_1 and \mathbf{u}_2 . If $\|\mathbf{u}_1\|$ is smaller than $\|\mathbf{u}_2\|$ but \mathbf{u}_1 is more aligned with its displacement, two scenarios arise:

1. For larger T , GALA selects layer 1, favoring the alignment and exploiting the learned direction. This scenario would seem more common during TTA.
2. For small T , GALA selects layer 2, favoring the magnitude, and can explore over different directions. This can occur for initial samples.

Consequently, GALA effectively balances the gradient magnitude and the direction of gradients for selecting the best layer. More discussion is in Appendix A.5.

Proposed layer selection framework offers a more flexible adaptation strategy for TTA. The selection of layers in existing TTA approaches typically remains unchanged across different shifts. On the other hand, sample selection-based TTA (Niu et al. 2022) approaches aim to improve performance by skipping the adaptation of all layers on a few unreliable samples. Based on Eq. 3 and Fig. 8, we can see that GALA is more flexible and general than the existing

layer selection and sample selection strategies in TTA for performing layerwise adaptation.

Reset mechanism seems beneficial in multi-domain shift settings. Comparing GALA with and without reset on Tab. 4, we see that while reset yields only marginal improvement on Domainbed, a single-domain shift benchmark, its benefits are more evident on a multi-shift benchmark like Continual TTA. This indicates that the reset mechanism’s ability to facilitate slight adjustments in the overall gradient update direction may be advantageous in a continuously changing testing domain.

GALA is quite robust on single sample adaptation. In Tab. 4, we show that in the adverse setting of batch size of 1, while existing TTA approaches witness severe performance degradation, GALA improves on *all layers* baseline on Domainbed.

6 Conclusion

In this paper, we introduce Gradient Aligned Layer Adaptation (GALA), a novel layer selection framework explicitly designed for Test Time Adaptation (TTA). Our comprehensive study reveals that layers in neural networks exhibit varying receptiveness to adaptation, and the optimal set of layers for adaptation depends on both the specific distribution shift and the loss function employed during inference. Building on these insights, we propose GALA, a dynamic layer selection criterion that ranks layers based on gradient alignment, effectively mitigating overfitting and performance degradation. Extensive experiments across diverse datasets, model architectures, and TTA losses demonstrate GALA’s superior performance compared to existing methods, including standard *ERM*, *all-layers* adaptation, and other layer selection baselines.

Acknowledgments

This work is supported by the DEEL Project CRDPJ 537462-18 funded by the Natural Sciences and Engineering Research Council of Canada (NSERC) and the Consortium for Research and Innovation in Aerospace in Québec (CRIAQ), together with its industrial partners Thales Canada inc, Bell Textron Canada Limited, CAE inc and Bombardier inc. ¹ Computations were made on the cedar, and beluga supercomputers, managed by Calcul Québec and the Digital Research Alliance of Canada (Alliance). We extend our gratitude to the members of the #lunch-at-mila and #deel.ood for their valuable input, with special thanks to Vineetha Kondameedi for her essential feedback in enhancing the quality of this paper.

References

- Agarwal, C.; D’souza, D.; and Hooker, S. 2022. Estimating example difficulty using variance of gradients. In *Proceedings of the IEEE/CVF Conference on Computer Vision and Pattern Recognition*, 10368–10378. [1](#), [2](#), [3](#), [13](#)
- Ahn, C.; Kim, E.; and Oh, S. 2019. Deep elastic networks with model selection for multi-task learning. In *Proceedings of the IEEE/CVF international conference on computer vision*, 6529–6538. [12](#)
- Andriushchenko, M.; and Flammarion, N. 2020. Understanding and improving fast adversarial training. *Advances in Neural Information Processing Systems*, 33: 16048–16059. [12](#)
- Bai, Y.; Yang, E.; Han, B.; Yang, Y.; Li, J.; Mao, Y.; Niu, G.; and Liu, T. 2021. Understanding and improving early stopping for learning with noisy labels. *Advances in Neural Information Processing Systems*, 34: 24392–24403. [13](#)
- Barba, L.; Jaggi, M.; and Dandi, Y. 2021. Implicit gradient alignment in distributed and federated learning. In *AAAI Conference on Artificial Intelligence*, AAAI, volume 22. [12](#)
- Beery, S.; Van Horn, G.; and Perona, P. 2018. Recognition in terra incognita. In *Proceedings of the European conference on computer vision (ECCV)*, 456–473. [4](#), [13](#)
- Bonet, D.; Ortega, A.; Ruiz-Hidalgo, J.; and Shekizhar, S. 2021. Channel-wise early stopping without a validation set via NNK polytope interpolation. In *2021 Asia-Pacific Signal and Information Processing Association Annual Summit and Conference (APSIPA ASC)*, 351–358. IEEE. [13](#)
- Bordes, F.; Balestriero, R.; Garrido, Q.; Bardes, A.; and Vincent, P. 2023. Guillotine Regularization: Why removing layers is needed to improve generalization in Self-Supervised Learning. *Transactions on Machine Learning Research*. [12](#)
- Boudiaf, M.; Mueller, R.; Ben Ayed, I.; and Bertinetto, L. 2022. Parameter-free online test-time adaptation. In *Proceedings of the IEEE/CVF Conference on Computer Vision and Pattern Recognition*, 8344–8353. [13](#)
- Burns, C.; and Steinhardt, J. 2021. Limitations of post-hoc feature alignment for robustness. In *Proceedings of the IEEE/CVF Conference on Computer Vision and Pattern Recognition*, 2525–2533. [1](#)
- Chattopadhyay, P.; Balaji, Y.; and Hoffman, J. 2020. Learning to Balance Specificity and Invariance for In and Out of Domain Generalization. In *European Conference in Computer Vision (ECCV)*. [1](#), [12](#)
- Chen, D.; Wang, D.; Darrell, T.; and Ebrahimi, S. 2022. Contrastive test-time adaptation. In *Proceedings of the IEEE/CVF Conference on Computer Vision and Pattern Recognition*, 295–305. [12](#)
- Choi, M. J.; Lim, J. J.; Torralba, A.; and Willsky, A. S. 2010. Exploiting hierarchical context on a large database of object categories. In *2010 IEEE computer society conference on computer vision and pattern recognition*, 129–136. IEEE. [13](#)
- Croce, F.; Andriushchenko, M.; Sehwag, V.; Debenedetti, E.; Flammarion, N.; Chiang, M.; Mittal, P.; and Hein, M. 2021. RobustBench: a standardized adversarial robustness benchmark. In *Thirty-fifth Conference on Neural Information Processing Systems Datasets and Benchmarks Track (Round 2)*. [4](#), [15](#)
- Darrin, M.; Staerman, G.; Gomes, E. D. C.; Cheung, J. C.; Piantanida, P.; and Colombo, P. 2024. Unsupervised layer-wise score aggregation for textual ood detection. In *Proceedings of the AAAI Conference on Artificial Intelligence*, volume 38, 17880–17888. [12](#)
- Du, Y.; Czarnecki, W. M.; Jayakumar, S. M.; Farajtabar, M.; Pascanu, R.; and Lakshminarayanan, B. 2018. Adapting auxiliary losses using gradient similarity. *arXiv preprint arXiv:1812.02224*. [13](#)
- ElAraby, M.; Sahoo, S.; Pequignot, Y.; Novello, P.; and Paull, L. 2023. GROOM: GRadient-aware Out-Of-Distribution detection in interpolated manifolds. *arXiv preprint arXiv:2312.14427*. [12](#)
- Everingham, M.; Van Gool, L.; Williams, C. K.; Winn, J.; and Zisserman, A. 2010. The pascal visual object classes (voc) challenge. *International journal of computer vision*, 88: 303–338. [13](#)
- Fang, C.; Xu, Y.; and Rockmore, D. N. 2013. Unbiased metric learning: On the utilization of multiple datasets and web images for softening bias. In *Proceedings of the IEEE International Conference on Computer Vision*, 1657–1664. [4](#), [13](#)
- Fei-Fei, L.; Fergus, R.; and Perona, P. 2004. Learning generative visual models from few training examples: An incremental bayesian approach tested on 101 object categories. In *2004 conference on computer vision and pattern recognition workshop*, 178–178. IEEE. [13](#)
- Forouzes, M.; and Thiran, P. 2021. Disparity between batches as a signal for early stopping. In *Machine Learning and Knowledge Discovery in Databases. Research Track: European Conference, ECML PKDD 2021, Bilbao, Spain, September 13–17, 2021, Proceedings, Part II 21*, 217–232. Springer. [1](#), [2](#), [3](#), [13](#)
- Fort, S.; Nowak, P. K.; Jastrzebski, S.; and Narayanan, S. 2019. Stiffness: A new perspective on generalization in neural networks. *arXiv preprint arXiv:1901.09491*. [13](#)
- Gao, J.; Zhang, J.; Liu, X.; Darrell, T.; Shelhamer, E.; and Wang, D. 2023. Back to the source: Diffusion-driven adaptation to test-time corruption. In *Proceedings of the IEEE/CVF*

¹<https://deel.quebec>

- Conference on Computer Vision and Pattern Recognition*, 11786–11796. [12](#)
- Gao, Z.; Zhang, S.; Huang, K.; Wang, Q.; and Zhong, C. 2021. Gradient distribution alignment certificates better adversarial domain adaptation. In *Proceedings of the IEEE/CVF international conference on computer vision*, 8937–8946. [12](#)
- Gauch, M.; Beck, M.; Adler, T.; Kotsur, D.; Fiel, S.; Eghbal-zadeh, H.; Brandstetter, J.; Kofler, J.; Holzleitner, M.; Zellinger, W.; et al. 2022. Few-shot learning by dimensionality reduction in gradient space. In *Conference on Lifelong Learning Agents*, 1043–1064. PMLR. [12](#)
- Gidaris, S.; Singh, P.; and Komodakis, N. 2018. Unsupervised representation learning by predicting image rotations. *arXiv preprint arXiv:1803.07728*. [12](#)
- Gong, T.; Jeong, J.; Kim, T.; Kim, Y.; Shin, J.; and Lee, S.-J. 2022. Note: Robust continual test-time adaptation against temporal correlation. *Advances in Neural Information Processing Systems*, 35: 27253–27266. [13](#)
- Gulrajani, I.; and Lopez-Paz, D. 2021. In Search of Lost Domain Generalization. In *International Conference on Learning Representations*. [1](#), [2](#), [3](#), [4](#), [13](#)
- Guo, P.; Lee, C.-Y.; and Ulbricht, D. 2020. Learning to branch for multi-task learning. In *International conference on machine learning*, 3854–3863. PMLR. [12](#)
- Guo, Y.; Shi, H.; Kumar, A.; Grauman, K.; Rosing, T.; and Feris, R. 2019. Spottune: transfer learning through adaptive fine-tuning. In *Proceedings of the IEEE/CVF conference on computer vision and pattern recognition*, 4805–4814. [12](#)
- Gupta, G.; Yadav, K.; and Paull, L. 2020. Look-ahead meta learning for continual learning. *Advances in Neural Information Processing Systems*, 33: 11588–11598. [13](#)
- Gur-Ari, G.; Roberts, D. A.; and Dyer, E. 2018. Gradient descent happens in a tiny subspace. *arXiv preprint arXiv:1812.04754*. [3](#), [12](#)
- Hendrycks, D.; and Dietterich, T. 2018. Benchmarking Neural Network Robustness to Common Corruptions and Perturbations. In *International Conference on Learning Representations*. [15](#)
- Hendrycks, D.; and Dietterich, T. 2019. Benchmarking neural network robustness to common corruptions and perturbations. In *International Conference on Learning Representations*. [4](#)
- Hu, X.; Zhang, K.; Sun, M.; Chen, A.; Kuo, C.-H.; and Nevatia, R. 2024. BaFTA: Backprop-Free Test-Time Adaptation For Zero-Shot Vision-Language Models. *arXiv preprint arXiv:2406.11309*. [12](#)
- Iwasawa, Y.; and Matsuo, Y. 2021. Test-time classifier adjustment module for model-agnostic domain generalization. *Advances in Neural Information Processing Systems*, 34: 2427–2440. [4](#), [12](#), [13](#), [14](#), [15](#), [16](#), [17](#)
- Jang, M.; Chung, S.-Y.; and Chung, H. W. 2023. Test-Time Adaptation via Self-Training with Nearest Neighbor Information. In *The Twelfth International Conference on Learning Representations*. [12](#), [13](#)
- Ji, Z.; and Telgarsky, M. 2020. Directional convergence and alignment in deep learning. In Larochelle, H.; Ranzato, M.; Hadsell, R.; Balcan, M.; and Lin, H., eds., *Advances in Neural Information Processing Systems*, volume 33, 17176–17186. Curran Associates, Inc. [12](#)
- Kim, E.; Sun, M.; Raghunathan, A.; and Kolter, Z. 2023. Reliable Test-Time Adaptation via Agreement-on-the-Line. *arXiv preprint arXiv:2310.04941*. [13](#)
- Kirichenko, P.; Izmailov, P.; and Wilson, A. G. 2023. Last Layer Re-Training is Sufficient for Robustness to Spurious Correlations. In *The Eleventh International Conference on Learning Representations*. [12](#)
- Krizhevsky, A.; Hinton, G.; et al. 2009. Learning multiple layers of features from tiny images. *Toronto, ON, Canada*. [15](#)
- Lee, A.; Bai, X.; Pres, I.; Wattenberg, M.; Kummerfeld, J. K.; and Mihalcea, R. 2024. A Mechanistic Understanding of Alignment Algorithms: A Case Study on DPO and Toxicity. In *Forty-first International Conference on Machine Learning*. [12](#)
- Lee, D.-H.; et al. 2013. Pseudo-label: The simple and efficient semi-supervised learning method for deep neural networks. In *Workshop on challenges in representation learning, ICML*, volume 3, 896. Atlanta. [3](#), [13](#), [15](#)
- Lee, Y.; Chen, A. S.; Tajwar, F.; Kumar, A.; Yao, H.; Liang, P.; and Finn, C. 2023. Surgical Fine-Tuning Improves Adaptation to Distribution Shifts. In *The Eleventh International Conference on Learning Representations*. [1](#), [2](#), [4](#), [5](#), [12](#), [14](#)
- Li, D.; Yang, Y.; Song, Y.-Z.; and Hospedales, T. M. 2017. Deeper, broader and artier domain generalization. In *Proceedings of the IEEE international conference on computer vision*, 5542–5550. [4](#), [13](#)
- Li, T.; Tan, L.; Tao, Q.; Liu, Y.; and Huang, X. 2021. Low dimensional landscape hypothesis is true: DNNs can be trained in tiny subspaces. *arXiv preprint arXiv:2103.11154*. [12](#)
- Liang, J.; He, R.; and Tan, T.-P. 2023. A Comprehensive Survey on Test-Time Adaptation under Distribution Shifts. *International Journal of Computer Vision*. [1](#), [2](#)
- Liang, J.; Hu, D.; and Feng, J. 2020. Do we really need to access the source data? source hypothesis transfer for unsupervised domain adaptation. In *International conference on machine learning*, 6028–6039. PMLR. [3](#), [13](#), [15](#)
- Lin, Z.; Roy, S. D.; and Li, Y. 2021. Mood: Multi-level out-of-distribution detection. In *Proceedings of the IEEE/CVF conference on Computer Vision and Pattern Recognition*, 15313–15323. [12](#)
- Liu, J.; Bai, Y.; Jiang, G.; Chen, T.; and Wang, H. 2020. Understanding Why Neural Networks Generalize Well Through GSNR of Parameters. In *International Conference on Learning Representations*. [12](#)
- Mahsereci, M.; Balles, L.; Lassner, C.; and Hennig, P. 2017. Early stopping without a validation set. *arXiv preprint arXiv:1703.09580*. [1](#), [2](#), [3](#), [13](#)
- Michalkiewicz, M.; Faraki, M.; Yu, X.; Chandraker, M.; and Baktashmotlagh, M. 2023. Domain Generalization

- Guided by Gradient Signal to Noise Ratio of Parameters. In *Proceedings of the IEEE/CVF International Conference on Computer Vision (ICCV)*, 6177–6188. [13](#)
- Murali, N.; Puli, A.; Yu, K.; Ranganath, R.; and Batmanghelich, K. 2023. Beyond Distribution Shift: Spurious Features Through the Lens of Training Dynamics. *Transactions on machine learning research*, 2023. [12](#)
- Niu, S.; Wu, J.; Zhang, Y.; Chen, Y.; Zheng, S.; Zhao, P.; and Tan, M. 2022. Efficient test-time model adaptation without forgetting. In *International conference on machine learning*, 16888–16905. PMLR. [1](#), [7](#), [12](#), [15](#)
- Niu, S.; Wu, J.; Zhang, Y.; Wen, Z.; Chen, Y.; Zhao, P.; and Tan, M. 2023. Towards Stable Test-time Adaptation in Dynamic Wild World. In *The Eleventh International Conference on Learning Representations*. [12](#)
- Panigrahi, A.; Saunshi, N.; Zhao, H.; and Arora, S. 2023. Task-Specific Skill Localization in Fine-tuned Language Models. In *International conference on machine learning*. PMLR. [12](#)
- Parascandolo, G.; Neitz, A.; Orvieto, A.; Gresele, L.; and Schölkopf, B. 2021. Learning explanations that are hard to vary. In *9th International Conference on Learning Representations, ICLR*. [13](#)
- Park, J.; Kim, J.; Kwon, H.; Yoon, I.; and Sohn, K. 2024. Layer-wise Auto-Weighting for Non-Stationary Test-Time Adaptation. In *Proceedings of the IEEE/CVF Winter Conference on Applications of Computer Vision*, 1414–1423. [12](#)
- Pasad, A.; Shi, B.; and Livescu, K. 2023. Comparative layer-wise analysis of self-supervised speech models. In *ICASSP 2023-2023 IEEE International Conference on Acoustics, Speech and Signal Processing (ICASSP)*, 1–5. IEEE. [12](#)
- Rajasegaran, J.; Hayat, M.; Khan, S. H.; Khan, F. S.; and Shao, L. 2019. Random path selection for continual learning. *Advances in neural information processing systems*, 32. [12](#)
- Russell, B. C.; Torralba, A.; Murphy, K. P.; and Freeman, W. T. 2008. LabelMe: a database and web-based tool for image annotation. *International journal of computer vision*, 77: 157–173. [13](#)
- Sankararaman, K. A.; De, S.; Xu, Z.; Huang, W. R.; and Goldstein, T. 2020. The impact of neural network overparameterization on gradient confusion and stochastic gradient descent. In *International conference on machine learning*, 8469–8479. PMLR. [12](#)
- Shi, Y.; Seely, J.; Torr, P. H. S.; Narayanaswamy, S.; Hannun, A. Y.; Usunier, N.; and Synnaeve, G. 2022. Gradient Matching for Domain Generalization. In *The Tenth International Conference on Learning Representations, ICLR*. [13](#)
- Shin, J.; Lee, J.; Lee, S.; Park, M.; Lee, D.; Hwang, U.; and Yoon, S. 2024. Gradient Alignment with Prototype Feature for Fully Test-time Adaptation. *arXiv preprint arXiv:2402.09004*. [1](#), [12](#)
- Sorrenti, A.; Bellitto, G.; Salanitri, F. P.; Pennisi, M.; Spampinato, C.; and Palazzo, S. 2023. Selective Freezing for Efficient Continual Learning. In *Proceedings of the IEEE/CVF International Conference on Computer Vision*, 3550–3559. [12](#)
- Su, Y.; Xu, X.; and Jia, K. 2022. Revisiting realistic test-time training: Sequential inference and adaptation by anchored clustering. *Advances in Neural Information Processing Systems*, 35: 17543–17555. [12](#)
- Sun, X.; Panda, R.; Feris, R.; and Saenko, K. 2020a. Adashare: Learning what to share for efficient deep multi-task learning. *Advances in Neural Information Processing Systems*, 33: 8728–8740. [12](#)
- Sun, Y.; Wang, X.; Liu, Z.; Miller, J.; Efros, A.; and Hardt, M. 2020b. Test-time training with self-supervision for generalization under distribution shifts. In *International conference on machine learning*, 9229–9248. PMLR. [2](#)
- Suteu, M.; and Guo, Y. 2019. Regularizing deep multi-task networks using orthogonal gradients. *arXiv preprint arXiv:1912.06844*. [13](#)
- Venkateswara, H.; Eusebio, J.; Chakraborty, S.; and Panchanathan, S. 2017. Deep hashing network for unsupervised domain adaptation. In *Proceedings of the IEEE conference on computer vision and pattern recognition*, 5018–5027. [4](#), [13](#)
- Vianna, P.; Chaudhary, M. S.; Tang, A.; Cloutier, G.; Wolf, G.; Eickenberg, M.; and Belilovsky, E. 2023. Channel Selection for Test-Time Adaptation Under Distribution Shift. *NeurIPS 2023 Workshop on Distribution Shifts: New Frontiers with Foundation Models*. [12](#)
- Wallingford, M.; Li, H.; Achille, A.; Ravichandran, A.; Fowlkes, C.; Bhotika, R.; and Soatto, S. 2022. Task adaptive parameter sharing for multi-task learning. In *Proceedings of the IEEE/CVF Conference on Computer Vision and Pattern Recognition*, 7561–7570. [1](#), [12](#)
- Wang, D.; Shelhamer, E.; Liu, S.; Olshausen, B.; and Darrell, T. 2020. Tent: Fully test-time adaptation by entropy minimization. *arXiv preprint arXiv:2006.10726*. [15](#)
- Wang, Q.; Fink, O.; Van Gool, L.; and Dai, D. 2022. Continual test-time domain adaptation. In *Proceedings of the IEEE/CVF Conference on Computer Vision and Pattern Recognition*, 7201–7211. [2](#), [4](#), [12](#), [14](#), [15](#)
- Wang, S.; Zhang, D.; Yan, Z.; Zhang, J.; and Li, R. 2023. Feature alignment and uniformity for test time adaptation. In *Proceedings of the IEEE/CVF Conference on Computer Vision and Pattern Recognition*, 20050–20060. [13](#)
- Wang, Z.; Luo, Y.; Zheng, L.; Chen, Z.; Wang, S.; and Huang, Z. 2024. In Search of Lost Online Test-time Adaptation: A Survey. *International Journal of Computer Vision (IJCV)*. [1](#)
- Wortsman, M.; Ilharco, G.; Gadre, S. Y.; Roelofs, R.; Gontijo-Lopes, R.; Morcos, A. S.; Namkoong, H.; Farhadi, A.; Carmon, Y.; Kornblith, S.; et al. 2022. Model soups: averaging weights of multiple fine-tuned models improves accuracy without increasing inference time. In *International Conference on Machine Learning*, 23965–23998. PMLR. [12](#)
- Wu, Y.; Wang, H.; Huang, L.-K.; Zheng, Y.; Zhao, P.; and Wei, Y. 2024a. Enhanced Gradient Aligned Continual Learning via Pareto Optimization. In *International Conference on Learning Representations*. [13](#)

- Wu, Y.; Wang, H.; Zhao, P.; Zheng, Y.; Wei, Y.; and Huang, L.-K. 2024b. Mitigating Catastrophic Forgetting in Online Continual Learning by Modeling Previous Task Interrelations via Pareto Optimization. In *Forty-first International Conference on Machine Learning*. 13
- Xie, S.; Girshick, R.; Dollár, P.; Tu, Z.; and He, K. 2017. Aggregated residual transformations for deep neural networks. In *Proceedings of the IEEE conference on computer vision and pattern recognition*, 1492–1500. 4, 15
- Yaras, C.; Wang, P.; Hu, W.; Zhu, Z.; Balzano, L.; and Qu, Q. 2023. The law of parsimony in gradient descent for learning deep linear networks. *arXiv preprint arXiv:2306.01154*. 12
- Yu, T.; Kumar, S.; Gupta, A.; Levine, S.; Hausman, K.; and Finn, C. 2020. Gradient surgery for multi-task learning. *Advances in Neural Information Processing Systems*, 33: 5824–5836. 13
- Yu, Y.; Shin, S.; Lee, S.; Jun, C.; and Lee, K. 2023. Block selection method for using feature norm in out-of-distribution detection. In *Proceedings of the IEEE/CVF Conference on Computer Vision and Pattern Recognition*, 15701–15711. 12
- Yuan, L.; Xie, B.; and Li, S. 2023. Robust test-time adaptation in dynamic scenarios. In *Proceedings of the IEEE/CVF Conference on Computer Vision and Pattern Recognition*, 15922–15932. 15
- Yuan, S.; Feng, L.; and Liu, T. 2024. Early Stopping Against Label Noise Without Validation Data. In *International Conference on Learning Representations*. 13
- Yuan, Y.; He, R.; Dong, Y.; Han, Z.; and Yin, Y. 2024. Discriminability-Driven Channel Selection for Out-of-Distribution Detection. In *Proceedings of the IEEE/CVF Conference on Computer Vision and Pattern Recognition*, 26171–26180. 12
- Zagoruyko, S.; and Komodakis, N. 2016. Wide Residual Networks. In *British Machine Vision Conference*. British Machine Vision Association. 4, 15
- Zhang, M.; Levine, S.; and Finn, C. 2022. Memo: Test time robustness via adaptation and augmentation. *Advances in Neural Information Processing Systems*, 35: 38629–38642. 12
- Zhang, W.; Wan, C.; Zhang, Y.; Cheung, Y.-m.; Tian, X.; Shen, X.; and Ye, J. 2024. Interpreting and Improving Large Language Models in Arithmetic Calculation. In *Forty-first International Conference on Machine Learning*. 12
- Zhang, Z.; Chen, W.; Cheng, H.; Li, Z.; Li, S.; Lin, L.; and Li, G. 2022. Divide and contrast: Source-free domain adaptation via adaptive contrastive learning. *Advances in Neural Information Processing Systems*, 35: 5137–5149. 12
- Zhao, B.; Chen, C.; and Xia, S.-T. 2023. DELTA: DEGRADATION-FREE FULLY TEST-TIME ADAPTATION. In *The Eleventh International Conference on Learning Representations*. 12
- Zhao, H.; Liu, Y.; Alahi, A.; and Lin, T. 2023a. On Pitfalls of Test-Time Adaptation. In *International conference on machine learning*. PMLR. 1, 3, 13, 18
- Zhao, H.; Zhou, T.; Long, G.; Jiang, J.; and Zhang, C. 2023b. Does continual learning equally forget all parameters? In *International Conference on Machine Learning*, 42280–42303. PMLR. 1, 12

Supplementary Materials for “A Layer Selection Approach to Test Time Adaptation”

In the supplementary section, we provide a comprehensive discussion of the experimental setups and the proposed approach, GALA. The supplementary material is organized as follows:

- **Sec. A.1:** Related works section.
- **Sec. A.2:** Implementation details of the Domainbed benchmark (for Tables 1, 4, and Figure 4).
- **Sec. A.3:** Implementation details of the Continual TTA benchmark (for Tables 2 and 4).
- **Sec. A.4:** Implementation details of the Tiny Domainbed benchmark (for Table 3), including the rationale for selecting critical shifts from the Domainbed benchmark.
- **Sec. A.5:** An in-depth discussion of GALA, including pseudocode and an analysis of its balance between gradient alignment and magnitude.
- **Sec. A.6:** Additional experimental result tables and plots not included in the main paper.
- **Sec. A.7:** Discussion section.

The numbering of figures, tables, and equations in this supplementary material continues from the main paper to ensure consistency and avoid repetition.

A.1 Related Works

A.1.1 Regularization in test time adaptation

Various regularization approaches have been proposed to address the problem of degradation in TTA. While few works try to improve the quality of pseudolabels used for adaptation (Chen et al. 2022; Wang et al. 2022), other set of works try to improve class prototypes (Iwasawa and Matsuo 2021; Jang, Chung, and Chung 2023; Hu et al. 2024). Constraining the model by aligning source and target domain features has also been explored in various works (Su, Xu, and Jia 2022; Zhang et al. 2022; Gao et al. 2023). Also, a lot of works have proposed different regularization terms to the TTA formulation to prevent degradation (Niu et al. 2022; Zhang, Levine, and Finn 2022; Zhao, Chen, and Xia 2023; Niu et al. 2023; Shin et al. 2024) However, in this paper, we take a parameter-centric approach to regularize test time adaptation, which we argue can be more effective for efficient TTA. Moreover, these regularization approaches can be used in conjunction with our proposed approaches to improve TTA performance further.

A.1.2 Layer selection

Layer selection or identifying the optimal set of parameters for a certain task has been important for a number of fields. Layer selection can help improve the performance in fine-tuning. Layer selection can improve sharing of features across different tasks which has been found to be beneficial in multi-task learning (Ahn, Kim, and Oh 2019; Guo, Lee, and Ulbricht 2020; Wallingford et al. 2022; Sun et al.

2020a), and continual learning (Rajasegaran et al. 2019; Sorrenti et al. 2023; Zhao et al. 2023b). While good layer selection can help us better understand and explain features learnt by the model (Lee et al. 2024; Zhang et al. 2024), identifying the right layer to take features from can be important for out-of-distribution detection (Lin, Roy, and Li 2021; Yu et al. 2023; ElAraby et al. 2023; Darrin et al. 2024; Yuan et al. 2024). In pretraining, layer selection can help create robust pretrained models for domain generalization (Chattopadhyay, Balaji, and Hoffman 2020), or can result in different amounts of performance gains in self supervised learning (Gidaris, Singh, and Komodakis 2018; Borges et al. 2023; Pasad, Shi, and Livescu 2023). Closer to our field, identifying the right set of parameters to train has shown to have big impacts in performance in fine-tuning (Guo et al. 2019; Wortsman et al. 2022; Lee et al. 2023; Panigrahi et al. 2023) and learning robust non-spurious features (Kirichenko, Izmailov, and Wilson 2023; Murali et al. 2023). There have been few works Vianna et al. (2023); Lee et al. (2023); Park et al. (2024) that study the differential impact of parameters on TTA but the impact of these studies on parameter selection is somewhat limited to individual TTA losses, rendering them non-exhaustive and potentially inapplicable to other TTA losses proposed in the past or future. On the other hand, we propose a gradient aligned layer adaptation framework for TTA, which is more flexible than existing layer selection strategies, and we demonstrate it improves performance across different TTA losses.

A.1.3 Gradient alignment studies

Gur-Ari, Roberts, and Dyer (2018) discuss the phenomenon of gradient descent occurring within a tiny subspace. Yaras et al. (2023) demonstrate the presence of a low-dimensional structure in learning dynamics. Li et al. (2021) reveal that neural networks can be effectively trained in lower-dimensional subspaces. Gauch et al. (2022) show that gradient descent within a tiny subspace enhances generalization in few-shot learning. Liu et al. (2020) indicate that a high gradient signal-to-noise ratio can lead to improved generalization in neural networks. Ji and Telgarsky (2020) find that the gradients of neural networks converge to a single direction. Sankararaman et al. (2020) show that gradient alignment accelerates the training speed of neural networks. Building upon these approaches, this paper proposes a novel cosine distance-based criterion for layer selection in the context of test-time adaptation.

A.1.4 Applications of gradient alignment

Andriushchenko and Flammarion (2020) and Gao et al. (2021) propose using gradient alignment as a regularizer for adversarial training. Barba, Jaggi, and Dandi (2021) apply gradient alignment within the context of federated learning.

Fort et al. (2019) demonstrate that gradient alignment can be useful for detecting overfitting. Gupta, Yadav, and Paull (2020), along with Wu et al. (2024b,a), show that gradient alignment can mitigate catastrophic forgetting in continual learning. Michalkiewicz et al. (2023), Parascandolo et al. (2021) and Shi et al. (2022) utilize gradient alignment for domain generalization. Yu et al. (2020) show that gradient alignment aids in multi-task learning, a finding supported by Du et al. (2018) and Suteu and Guo (2019). Building on these approaches, we propose a novel formulation of gradient alignment for an online and unsupervised application of test time adaptation.

A.1.5 Gradient alignment-based early stopping

Recent works have proposed various approaches or criteria for early stopping without a validation set. Mahsereci et al. (2017) introduced an evidence-based criterion based on the variance of gradients (Agarwal, D’souza, and Hooker 2022). Forouzesh and Thiran (2021) proposed using gradient disparity across samples as a criterion. Yuan, Feng, and Liu (2024) suggested performing early stopping by tracking the model’s predictions on the samples. Most of these existing works have demonstrated the effectiveness of their proposed approaches, often in the context of multi-epoch and supervised learning (Bonet et al. 2021) or noisy learning (Bai et al. 2021). Similar to these approaches, our novel cosine distance-based criterion can be used to perform layer-wise early stopping without a validation set, preventing degradation in test-time adaptation and beyond.

A.2 Experimental Details of Domainbed

A.2.1 Dataset Details

Domainbed (Gulrajani and Lopez-Paz 2021) consists of four domain generalization datasets:

- PACS (Li et al. 2017) consists of different object images from four domains: Art, Cartoon, Photo, and Sketch. It comprises of 9,991 samples across 7 class labels (i.e., dog, elephant, giraffe, guitar, horse, house, and person).
- VLCS (Fang, Xu, and Rockmore 2013) consists of photographic images from four domains/datasets: PASCAL VOC207 (Everingham et al. 2010), LabelMe (Russell et al. 2008), Caltech 101 (Fei-Fei, Fergus, and Perona 2004), and SUN09(Choi et al. 2010). It comprises of 10,729 samples across 5 class labels (i.e., bird, car, chair, dog, and person).
- TerraIncognita (Beery, Van Horn, and Perona 2018) consists of images of wild animals taken at different locations, which make up the four domains: L100, L38, L43, and L46. It comprises of 24,788 samples across 10 class labels (i.e., bird, bobcat, cat, coyote, dog, empty/no animal, opossum, rabbit, raccoon, squirrel).
- Office-Home (Venkateswara et al. 2017) consists of different object images typically seen in offices and homes from four domains: Art, Clipart, Product, and Real World. It comprises of 15,588 samples across 65 class labels (e.g., bottle, computer, hammer, pen).

A.2.2 Evaluation Details

We follow the evaluation protocol as described in Iwasawa and Matsuo (2021). In Domainbed, the pretrained model is trained on all but one domain. All the domains on which the pretrained model is trained are referred to as training domains, and the remaining domain is referred to as the testing domain. We follow the dataset splits used in T3A (Iwasawa and Matsuo 2021). Each domain is split into a big and a small split. Specifically, the domains are split into 80% and 20%. The big split of training domains is used for training the pretrained model and is referred to as training splits. The small splits of training domains are referred to as validation splits. The big split of the testing domain is used to evaluate the domain and is referred to as the testing split. This is the split where test time adaptation is performed for each minibatch before inference. We consider three seeds for the results in Tab. 1 and one seed in Tab. 4, Fig. 4, and Fig. 6. Each seed generates a new training and testing split from training and testing domains. See Figure 1 “Data configuration for a benchmark with four domains” in Domainbed (Gulrajani and Lopez-Paz 2021) supplementary.

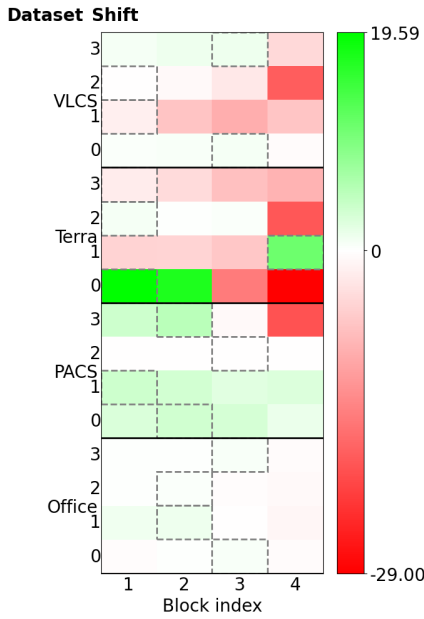
The performance on each domain or shift is obtained by averaging across multiple seeds. Next, we obtain the performance on each dataset by averaging across all domains in the dataset. Finally, we get performance on Domainbed by averaging across all the datasets in Domainbed.

A.2.3 Hyperparameters and Model Selection

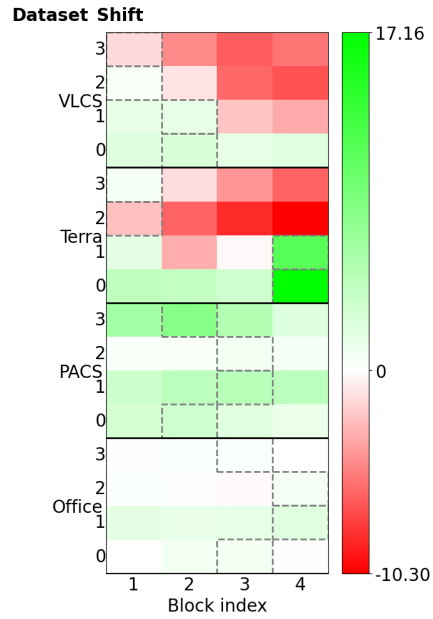
Pretrained Model We follow the pretraining protocol as described in Iwasawa and Matsuo (2021). We use ERM for pretraining the model similar to other works in TTA (Iwasawa and Matsuo 2021; Jang, Chung, and Chung 2023; Wang et al. 2023). We consider two backbones: Resnet-18 and Resnet-50, with batch normalization layers. The backbone networks are trained using ERM and Adam optimizer with a batch size of 32. We follow the training-domain validation-based model selection (Gulrajani and Lopez-Paz 2021; Iwasawa and Matsuo 2021) where we choose the hyperparameters that maximize the accuracy of the pretrained model on the validation splits. Please refer to Domainbed (Gulrajani and Lopez-Paz 2021) and T3A (Iwasawa and Matsuo 2021) for a detailed discussion on hyperparameters and the range used.

TTA Approaches We follow the adaptation protocol as described in Iwasawa and Matsuo (2021). Similar to other works in TTA (Zhao et al. 2023a; Kim et al. 2023; Boudiaf et al. 2022; Gong et al. 2022), our hyperparameter tuning protocol of TTA methods is based on Zhao et al. (2023a), where we choose the best hyperparameter set for each TTA method under consideration. We consider two popular TTA methods from Iwasawa and Matsuo (2021): pseudo-labeling (PL) (Lee et al. 2013) and SHOT (Liang, Hu, and Feng 2020). Please refer to Iwasawa and Matsuo (2021) for a detailed discussion on hyperparameters and the range used.

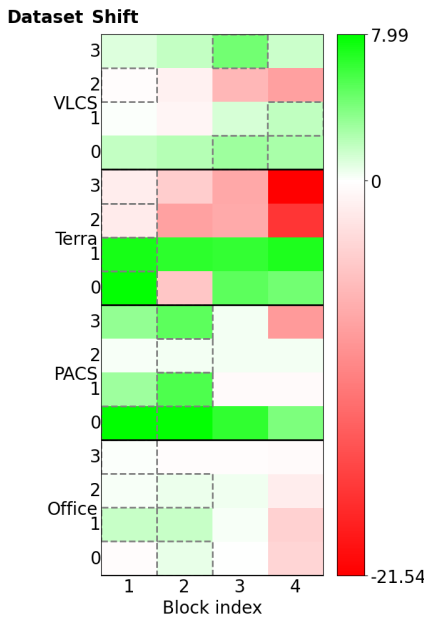
Baseline Layer Selection Methods We perform a model selection for each baseline as described in the original implementations. ERM (Gulrajani and Lopez-Paz 2021; Iwasawa



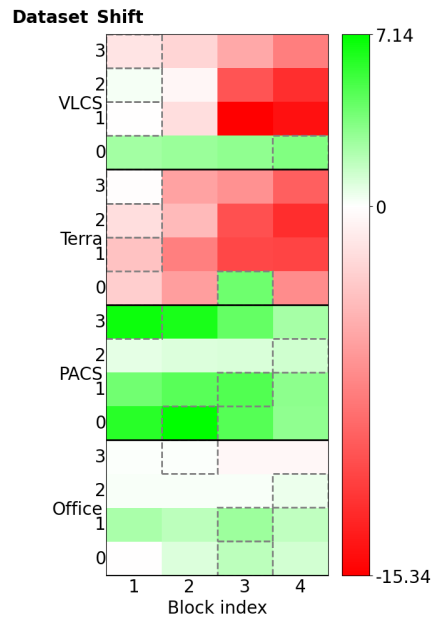
(a) Resnet-18 with PL loss



(b) Resnet-18 with SHOT loss



(c) Resnet-50 with PL loss



(d) Resnet-50 with SHOT loss

Figure 6: Heatmap of Performance improvement (%) per-block on Domainbed benchmark for Resnet-18 (same as Figure 4) and Resnet-50. Performance improvement is the difference between the TTA accuracy of a given block/layer and ERM accuracy for the same shift. Positive performance improvements are shown in green, and negative performance improvements (or degradation) are in red. Using the bounding box, we highlight the best block per loss and dataset shift.

and Matsuo 2021), *All Layers* (Iwasawa and Matsuo 2021), and AutoRGN (Lee et al. 2023) baselines do not have any hyperparameters. The hyperparameter for AutoSNR (Lee et al. 2023) baseline is tuned as described in Lee et al. (2023).

A.3 Experimental Details of Continual TTA

A.3.1 Dataset Details

Continual TTA benchmark (Wang et al. 2022) consists of two datasets, CIFAR10-C and CIFAR100-C, widely used for evaluating the robustness of classification networks un-

Algorithm 1: Gradient-Aligned Layer Adaptation (GALA)

```
1: Initialization: Pretrained model:  $f_{\theta_0}(x)$ , Anchor model
   parameters:  $\theta_{\text{anchor}} = \theta_0$ , Adaptation method: TTA,
   Window size:  $s$ , Mask threshold:  $\lambda$ 
2: Input for step  $i$ : Sample  $x_i$ , anchor  $\theta_{\text{anchor}}$  and current
   model  $\theta_{i-1}$ 
3:  $\mathbf{u}_i = \text{TTA}(x_i, \theta_{i-1})$ 
4: for each layer  $l$  do
5:    $\mathbf{TD}_{i-1,l} = \theta_{i-1,l} - \theta_{\text{anchor},l}$ 
6:    $\cos(\alpha_{i,l}) = \frac{\mathbf{u}_{i,l} \cdot (\mathbf{u}_{i,l} + \mathbf{TD}_{i-1,l})}{\|\mathbf{u}_{i,l}\|_2 \|\mathbf{u}_{i,l} + \mathbf{TD}_{i-1,l}\|_2}$ 
7:    $m_{i,l} = \begin{cases} 1 & \text{if } \cos(\alpha_{i,l}) > \lambda \\ 0 & \text{otherwise} \end{cases}$ 
8:    $\theta_{i,l} = \theta_{i-1,l} + m_{i,l} \mathbf{u}_{i,l}$ 
9: end for
10:  $r = \lfloor (i-1)/s \rfloor$ 
11: if  $i == r * s$  then
12:    $\theta_{\text{anchor}} = \theta_i$ 
13: end if
14: Output at step  $i$ : Prediction  $f_{\theta_i}(x_i)$ , Updated model
    $f_{\theta_i}$ 
```

der various corruptions, particularly in the context of test-time adaptation (TTA). These datasets are derived from the original CIFAR10 and CIFAR100 (Krizhevsky, Hinton et al. 2009), which contain 50,000 training and 10,000 test images across 10 and 100 categories, respectively. In CIFAR10-C and CIFAR100-C (Hendrycks and Dietterich 2018), 15 types of corruptions, each with 5 levels of severity, are applied to the test images of their clean counterparts. This results in 10,000 corrupted images for each corruption type in both the datasets.

A.3.2 Evaluation Details

We follow the evaluation protocol as described in Wang et al. (2022). We utilize a model pre-trained on the clean training set of the CIFAR10 or CIFAR100 dataset. During test time, corrupted images are provided to the network in an online fashion. We continually adapt the source pretrained model to each corruption type sequentially without resetting to the pretrained model. The CIFAR10 and CIFAR100 experiments follow this online continual test-time adaptation scheme, with evaluations conducted under the highest corruption severity level 5. The evaluation is based on the online prediction results immediately after encountering the data.

A.3.3 Hyperparameters and Model Selection

Pretrained Model We follow the pretraining protocol as described in Wang et al. (2022). For our experiments on CIFAR10C and CIFAR100C, we utilize pre-trained models from the RobustBench benchmark (Croce et al. 2021) similar to previous works in test time adaptation (Wang et al. 2020, 2022; Niu et al. 2022; Yuan, Xie, and Li 2023). Specifically, for CIFAR10C, we employ a WideResNet-28 (Zagoruyko and Komodakis 2016) model, and for CIFAR100C, we adopt a pre-trained ResNeXt-29 (Xie et al.

2017) model, which is one of the default architectures for CIFAR100 in RobustBench.

TTA Approaches We follow the evaluation protocol as described in Wang et al. (2022). We update the model with one gradient step per test point at each iteration, utilizing the Adam optimizer with a learning rate of 1e-3. The hyperparameters employed are consistent with those recommended by Wang et al. (2022). To facilitate comparison with Domainbed benchmark results, we incorporate the same two test-time adaptation methods: pseudo-labeling (PL) (Lee et al. 2013) and SHOT (Liang, Hu, and Feng 2020).

Baseline Layer Selection Methods We perform a model selection for each baseline as described in the original implementations. ERM (Croce et al. 2021; Wang et al. 2022) and *All Layers* (Iwasawa and Matsuo 2021) baselines do not have any hyperparameters.

A.4 Experimental Details of Tiny Domainbed

A.4.1 Dataset and Shift Details

We create Tiny-Domainbed from Domainbed by selecting the following critical shifts:

- Three shifts from the Terra Incognita benchmark: L100, L38, and L43;
- Two shifts from the PACS benchmark: Cartoon and Sketch;
- One shift from the VLCS benchmark: SUN09.

A.4.2 Discussion on Chosen Shifts

Creating Tiny-Domainbed aims to make the smallest possible setup of Domainbed, which contains all the challenging shifts or domains in Domainbed while being computationally light for ease of analysis and comparison. To identify the critical shifts of Domainbed, we refer to the heatmap of performance improvement of blocks vs. shifts in Domainbed in Fig. 6. We refer to blocks and layers interchangeably in this section.

Based on heatmaps of the Resnet-18 backbone for pseudolabelling and SHOT loss-based TTA methods in Fig. 6, we identify the critical shifts in Domainbed which satisfy the following two important properties:

- **Property 1: Shifts with brightest green/red blocks.** A bright green layer implies that adapting this layer improves performance over ERM. Similarly, a bright red layer implies that adapting this layer can degrade the performance with respect to ERM. The shifts with the brightest green or red layers are important because any layer selection criterion must do well on these shifts. The inability to choose bright green layers while adapting to these shifts is a missed opportunity for performance improvement of the layer selection approach. Again, being unable to avoid bright red layers in these shifts can result in significant performance degradation. In Fig. 6, we see that the following shifts on the Resnet-18 backbone have the brightest green/red layers: *env0, env1, env3* in PACS; *env2, env3* in VLCS; *env0, env1, env2, env3* in Terra Incognita; *none* in OfficeHome.

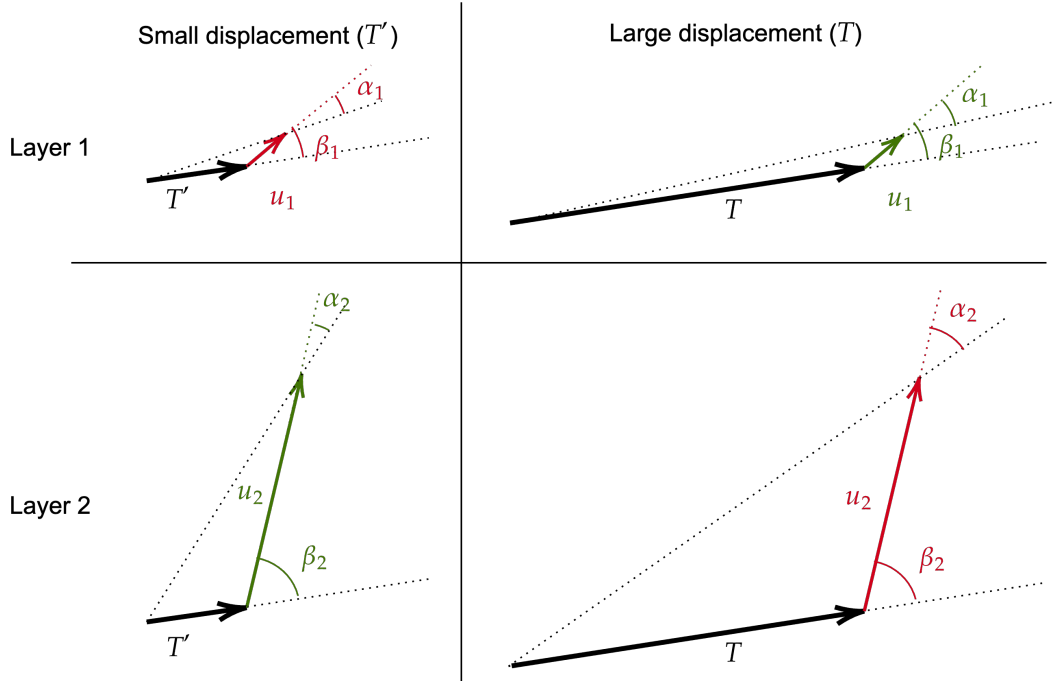


Figure 7: Effect of magnitude of \mathbf{u} on cosine distance criterion. Consider two vectors such that u_1 is smaller than u_2 but is better aligned with its displacement. The rows illustrate the layers, and the columns denote the two scenarios. The vectors are shown in green if the cosine distance selects the layer, or else shown in red. **Left:** In scenario 2 of small displacements (T'), the update’s magnitude can dominate the criterion, and GALA selects u_1 . **Right:** In scenario 1 of large displacements (T), alignment becomes crucial, and GALA selects u_2 .

- **Property 2: Shifts whose best block changes with the TTA loss function.** We make a striking observation that for certain shifts in Domainbed, the best block for a given shift can depend on the TTA loss used. This implies that the layer selection criterion must consider TTA loss to choose the best layers to adapt. In Fig. 6, we see that the following shifts on the Resnet-18 backbone experience a change in the location of the best block due to a change in the TTA method: *env1* in PACS; *env0*, *env3* in VLCS; *env0* in Terra Incognita; *env1*, *env2* in Office-Home.

To create the Tiny-Domainbed benchmark, we select the most critical shifts with the brightest green/red blocks, and the location of the best block changes with the TTA loss function. Based on this, we identify the following shifts from Domainbed to be included in the Tiny-Domainbed benchmark:

- Shifts that satisfy both the properties: *env3* in PACS; *env3* in VLCS; *env0* in Terra Incognita.
- Shifts that only satisfy property 1 but are included in Tiny Domainbed: *env1* in PACS; *env1*, *env2* in Terra Incognita.

This gives us our final list of critical shifts from Domainbed included in the Tiny-Domainbed benchmark: three

shifts from the Terra Incognita benchmark: L100, L38, and L43; two shifts from the PACS benchmark: Cartoon and Sketch, and one shift from the VLCS benchmark: SUN09.

A.4.3 Evaluation Details

We follow the evaluation protocol as described in Iwasawa and Matsuo (2021) and is described in detail in Sec. A.2.2. We obtain the performance on a given testing domain similar to the evaluation protocol of Domainbed. However, we obtain the final performance on Tiny-Domainbed by averaging across only the selected domains or shifts (identified as critical shifts in Sec. A.4.1) on the Resnet-18 backbone and two TTA losses.

Evaluation Metrics. We will explain the various metrics employed to compare different block or layer selection methods, as used in Table 3:

- **TTA Accuracy:** We abbreviate it as *TTA acc*. It refers to the accuracy of testing samples from the target domain observed during adaptation. This metric follows the same evaluation protocol as in Tables 1 and 2 to generate the TTA results, providing insight into the performance of different layer selection approaches at test time.
- **Generalization:** It measures the accuracy on the held-out split of the target domain after the model has completed adaptation on all the samples from the same target

Setting	Condition	Resnet-18 \uparrow		Resnet-50 \uparrow	
		PL	SHOT	PL	SHOT
Partitioning	Single block	66.19	65.8	70.21	68.37
	Single layer	66.31	66.78	71.07	70.13
	Multiple layers	63.13	65.36	69.11	68.29
Threshold	0.5	66.31	66.78	71.07	70.13
	0.75	66.31	66.78	71.07	70.13
	0.99	66.24	66.96	71.07	70.13
Window Size	5	66.37	66.61	70.87	70.01
	20	66.31	66.78	71.07	70.13
	∞	65.71	66.59	70.76	70.42
Batch Size = 1	All Layers	37.47	29.67	33.93	32.81
	GALA	64.12	64.29	70.45	70.24

Table 5: Accuracy (%) under different experimental conditions. The values are averaged for each backbone and TTA loss of the Domainbed benchmark.

domain. This metric indicates how each layer selection method aids in adapting the model to the target domain.

- **Forgetting:** This metric quantifies the drop in accuracy on the held-out split of source domains after the pre-trained model has adapted to all samples of the target domain, which differs from the source domains on which the pretrained model was initially trained. This metric helps us assess the degree of forgetting of source features due to various layer selection methods.
- **Rank Correlation:** In this metric, we measure the Spearman correlation of layer selection ranks between the oracle and proposed layer selection methods. Oracle TTA performance, as depicted in Figure 6, ranks the four blocks for each configuration. Similarly, different layer selection methods adapt a layer with a specific frequency during TTA, resulting in a ranking of the four blocks. We evaluate the relationship between these two ranking methods using Spearman rank correlation. This correlation provides insight into how well the proposed layer selection methods’ ranking of layers aligns with the oracle ranking on Tiny-Domainbed.

A.4.4 Hyperparameters and Model Selection

We follow the model selection and hyperparameter tuning protocol for pretrained models and TTA approaches as described in Iwasawa and Matsuo (2021) and is described in detail Sec. A.2.3. We consider only the Resnet-18 backbone with the batch normalization layers for ease of analysis. We consider two TTA losses: pseudolabelling and SHOT. We use *Block* granularity-based layer selection and report results for a single seed for easy analysis. Please note that although we perform block-based layer selection in Tiny-Domainbed, we interchangeably refer to block selection or layer selection in this section.

Layer Selection Methods. In Table 3, we compare the GALA method with the following oracle (*Best Block* and *Worst Block*) and baseline methods (All Blocks and Random Block):

- **All Blocks:** This is analogous to the *All Layers* baseline in Tables 1 and 2, where all blocks of the model are adapted at each adaptation step.

Setting	Condition	CIFAR10C \uparrow		CIFAR100C \uparrow	
		PL	SHOT	PL	SHOT
Continual TTA	No Reset	73.6	76.41	64.75	64.87
	With Reset	71.32	79.54	66.31	67.13

Table 6: Accuracy (%) under different experimental conditions. The values are averaged for each dataset and TTA loss of the Continual TTA benchmark.

- **Random Block:** During each adaptation step for a given sample, a block is chosen at random and adapted accordingly.
- **Best Block:** In this oracle layer selection method, the best-performing block for each shift and loss function, as identified in Figure 6, is adapted for all adaptation steps of the model.
- **Worst Block:** This oracle method adapts the worst-performing block for each shift and loss function, as identified in Figure 6, for all adaptation steps of the model.

A.5 Discussion on GALA

A.5.1 Pseudocode

A pseudocode of GALA is given in Algorithm 1.

A.5.2 Implementation details of GALA

GALA has two hyperparameters, namely *window size* and *mask threshold*. In Sec. 5, we show that GALA is not overly sensitive to its hyperparameters and, therefore, use a fixed value (*window size* = 20 and *mask threshold* = 0.75) across all setups when comparing with the baselines. Total displacement computed over the initial few samples may be unreliable, which can result in incorrect layers selected for adaptation. We address this by scaling the masked updates for an initial few samples in the reset window. One could also use an earlier anchor model from the previous reset window, but scaling the mask for a few initial minibatches seems to suffice.

Based on Sec. 5, we note that GALA performs the best when the pretrained model is adapted only with the best single layer identified by GALA (the one with the largest cosine distance above the selection threshold) but not with multiple or the top k -best layers identified by GALA (i.e., layers whose cosine distance is larger than the selection threshold). Therefore, we use GALA with Single-layer partitioning across all setups when comparing with the baselines. An important point to note is that GALA adapts all the layers for the first sample in a reset window. It adapts the most gradient-aligned layer per sample for all the other samples. (However, in the Tiny-Domainbed benchmark, we use Single-block partitioning since the analysis is performed at Block granularity.)

Since GALA performs the best with Single-layer partitioning instead of Multi-layer partitioning, it implies that GALA can often identify a good layer to adapt but may not identify all the top k -best layers to adapt above the selection threshold. This can be viewed as one of the limitations

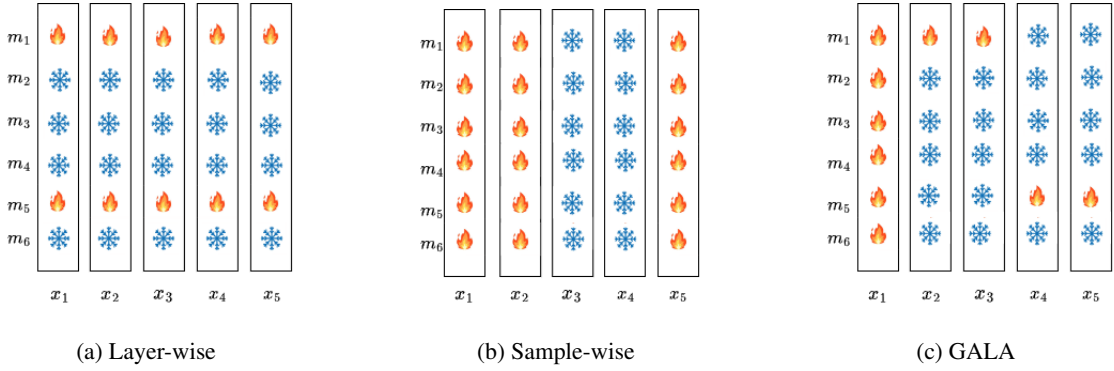


Figure 8: Different adaptation strategies: (a) TTA approaches typically adapt a fixed set of layers for all the samples. (b) Sample selection-based TTA approaches skip the adaptation of all layers on a few unreliable samples. (c) GALA is more flexible and can dynamically control the adaptation of individual layers per sample.

of GALA and can potentially be a fruitful research direction for future works. We note that one can address this limitation by tuning the hyperparameters of GALA (especially *mask threshold*) in each setup, similar to the recommendation made by Zhao et al. (2023a). However, we avoid any hyperparameter tuning of GALA in the paper and show that adapting the model with the best single-layer identified by GALA can outperform existing baselines.

A.5.3 Relationship between GALA and Eq. 8

For notational simplicity, we rewrite the following terms

- $\mathbf{u} = \mathbf{u}_{i,l}$, the current sample’s update for layer l .
- $u = \|\mathbf{u}\|_2$, the magnitude of the current sample’s update.
- $\mathbf{T} = \mathbf{T}\mathbf{D}_{i-1,l}$, the total displacement undergone in previous steps by layer l .
- $T = \|\mathbf{T}\|_2$, the magnitude of the total displacement. This is the *magnitude* used in Sec. 5 and Sec. A.5.4.
- $\beta = \beta_{i,l}$ is the angle between \mathbf{u} and \mathbf{T} .
- $\cos(\beta)$ is the alignment of \mathbf{u} with \mathbf{T} . This is the *alignment* used in Sec. 5 and Sec. A.5.4. We also interchangeably refer to it as *direction* since β is the angle \mathbf{u} makes with \mathbf{T} .
- $\alpha = \alpha_{i,l}$ is the angle between \mathbf{u} and $\mathbf{u} + \mathbf{T}$.
- $\cos(\alpha)$ is the proposed criterion of GALA. In Sec. 5 and Sec. A.5.4, we note that the proposed cosine distance criterion effectively balances *magnitude* and *alignment*.

Based on the above definitions, the *alignment* is given by

$$\cos(\beta) = \frac{\mathbf{u} \cdot \mathbf{T}}{u T} \quad (9)$$

Let us begin by expanding the numerator of Eq. 5,

$$\cos(\alpha) = \frac{\mathbf{u} \cdot (\mathbf{T} + \mathbf{u})}{u \|\mathbf{T} + \mathbf{u}\|_2} \quad (10)$$

$$= \frac{\mathbf{u} \cdot \mathbf{T} + \mathbf{u} \cdot \mathbf{u}}{u \|\mathbf{T} + \mathbf{u}\|_2} \quad (11)$$

$$= \frac{uT \cos(\beta) + u^2}{u \|\mathbf{T} + \mathbf{u}\|_2} \quad (12)$$

$$= \frac{T \cos(\beta) + u}{\|\mathbf{T} + \mathbf{u}\|_2} \quad (13)$$

If β is acute, then we can see that using the Pythagorean theorem, we get $\|\mathbf{T} + \mathbf{u}\|_2 = \sqrt{(T + u \cos(\beta))^2 + (u \sin(\beta))^2}$. One can show that this also holds for obtuse β , in which case $u \cos(\beta)$ is negative. Substituting this in the equation above, we get our Eq. 8 as

$$\cos(\alpha) = \frac{T \cos(\beta) + u}{\sqrt{(T + u \cos(\beta))^2 + (u \sin(\beta))^2}}. \quad (14)$$

A.5.4 Alignment vs Magnitude in GALA

In this section, we expand on the discussion of Sec. 5 to better understand how the proposed cosine distance criterion depends on the *magnitude* and the *alignment* of the current sample’s update with respect to the total displacement made so far.

From Eq. 14, it is clear that computing the proposed cosine distance criterion for a given layer only involves T , u , and the angle β . This means that even though the layers may have a considerable number of parameters, we can always draw a diagram like the ones in Fig. 7 to represent the situation and compare the updates for performing layer selection.

To better understand the interaction between magnitude and alignment towards cosine metric, we consider an example where we have two layers, layer 1 and layer 2, and their corresponding total displacement has the same norm T . We consider an update \mathbf{u}_1 for layer 1 and an update \mathbf{u}_2 for layer 2 with: $u_1 < u_2$. While the update for layer 2 has a larger

magnitude, the update \mathbf{u}_1 of layer 1 is more aligned with its displacement ($\beta_1 < \beta_2$). We observe that two scenarios can arise depending on the magnitude of the total displacement:

- **Scenario 1 of large T :** In this scenario, Cosine distance significantly depends on the *alignment* of the current sample and is less impacted by its *magnitude*. This scenario is more likely for most of the samples during TTA. This can also be viewed similarly to performing an exploit strategy in a given update direction, i.e., after having seen a certain number of samples, we allow adaptation of a layer if the gradients for new updates are well aligned with the previously seen updates.
- **Scenario 2 of small T :** In this scenario, Cosine distance significantly depends on the *magnitude* of the current sample and is less impacted by its *alignment* with the total displacement. This can occur for the very first samples in a few cases or if the gradients on a layer for a particular sample are much larger than usual. Similarly, we can view it as performing a form of pure exploration strategy over the update directions.

Fig. 5 (left) and Fig. 7 visualize the two scenarios for the above example.

A.6 Additional Experimental Results

In this section, we include the following additional experimental results not included in the main paper:

- **Performance improvement heatmap for Resnet-50 backbone on Domainbed benchmark:** While Fig. 4 shows the heatmap for performance improvement only for the Resnet-18 backbone, in Fig. 6, we also show the heatmap for performance improvement for the Resnet-50 backbone for comparison. Similar to the heatmap for Resnet-18, we observe that no single layer of Resnet-50 is suitable for all settings, and not all layers are equally receptive to adaptation. Moreover, similar to the Resnet-18’s backbone, we observe that the location of good layers can change across the shifts of a given dataset and for a TTA loss function even for the same shift.
- **Effect of experimental conditions on different backbones and TTA loss functions on Domainbed benchmark:** While the first four settings of Table 4 show the effect of experimental conditions averaged on the whole of Domainbed, Tab. 5 shows a more fine-grained impact of experimental conditions by reporting the values averaged on each backbone and TTA loss function of the Domainbed. Similar to the discussion in Sec. 5, we observe that Layer granularity performs better than Block granularity, and adaptation with the best Single-layer is much better than with the best Multiple-layers. Tuning the reset window size can improve performance, and the choice of selection threshold is not very sensitive. Finally, GALA improves over *All Layers* baseline on the single sample adaptation setting (with batch size = 1).
- **Effect of reset on different datasets of Continual TTA benchmark:** While the last setting of Tab. 4 shows the effect of reset averaged on the whole of Continual TTA,

Tab. 6 shows a more fine-grained effect of reset by reporting the values averaged on each dataset and TTA loss function of the Continual TTA. Our observations indicate that the GALA, when utilizing a reset mechanism with a window size of 20, is advantageous in most scenarios. While it does not appear to benefit the CIFAR10C dataset with PL loss-based TTA, tuning the reset window size could help improve the performance of the reset mechanism.

A.7 Discussion

The simplicity and versatility of GALA enable seamless integration with existing TTA loss functions, making it a valuable tool for enhancing the adaptability and reliability of deep learning models in real-world applications. Beyond its immediate impact on TTA, our work opens up new avenues for future research in areas where regularization is crucial for learning stability, selective parameter updates could be beneficial, or gradient-aligned feature learning might offer additional advantages. GALA not only advances the field of TTA but also contributes to the broader goal of developing more robust and adaptive AI systems.